Toxin Reviews

ISSN: 1556-9543 (Print) 1556-9551 (Online) Journal homepage: www.tandfonline.com/journals/itxr20

Biosynthesis, characterization, and insecticidal toxicity of iron oxide (Fe_2O_3) nanoparticles synthesized from marine macroalgae (*Ulva lactuca*)

Ramya Suseenthar, Palanivelan Ramachandran, Muthusamy Ranganathan, Mathiyazhagan Narayanasamy, Ramkumar Govindaraju, Prakash Balu & Nivetha Muthuganesh

To cite this article: Ramya Suseenthar, Palanivelan Ramachandran, Muthusamy Ranganathan, Mathiyazhagan Narayanasamy, Ramkumar Govindaraju, Prakash Balu & Nivetha Muthuganesh (23 Aug 2025): Biosynthesis, characterization, and insecticidal toxicity of iron oxide (Fe_2O_3) nanoparticles synthesized from marine macroalgae (*Ulva lactuca*), Toxin Reviews, DOI: 10.1080/15569543.2025.2548215

To link to this article: https://doi.org/10.1080/15569543.2025.2548215

Published online: 23 Aug 2025.

TOXIN REVIEWS
https://doi.org/10.1080/15569543.2025.2548215

Taylor & Francis
Taylor & Francis Group

RESEARCH ARTICLE

Check for updates

Biosynthesis, characterization, and insecticidal toxicity of iron oxide (Fe_2O_3) nanoparticles synthesized from marine macroalgae (*Ulva lactuca*)

Ramya Suseenthar[a], Palanivelan Ramachandran[b], Muthusamy Ranganathan[c], Mathiyazhagan Narayanasamy[d], Ramkumar Govindaraju[e], Prakash Balu[f] and Nivetha Muthuganesh[f]

[a]Department of Microbiology, MGR College, Hosur, Tamil Nadu, India; [b]Department of Microbiology, Indfrag Biosciences Pvt Ltd, Hosur, Tamil Nadu, India; [c]PG and Research Centre in Biotechnology, MGR College, Adhiyamaan Educational Research Institution, Hosur, Tamil Nadu, India; [d]Department of Agriculture Biotechnology, Faculty of Science, Tanta University, Tanta, Egypt; [e]College of Agricultural and Environmental Sciences, Department of Entomology, University of Georgia, Griffin, GA, USA; [f]Department of Biotechnology, School of Life Sciences, Vels Institute of Science, Technology and Advanced Studies (VISTAS), Chennai, India

ABSTRACT

Background and aim: The use of synthetic pesticides presents environmental and health hazards, necessitating the development of environmentally sustainable alternatives. This study seeks to synthesize and assess the insecticidal effectiveness of iron oxide nanoparticles obtained from the green seaweed *Ulva lactuca* against different instars of lepidopteran and dipteran insects.
Experimental approach: The synthesis of Fe_2O_3 nanoparticles was conducted via *U. lactuca* extract, followed by characterization via FTIR, XRD, TEM, SEM, and EDS studies. Larvicidal bioassays were performed at concentrations between 50 and 200 µg/mL for 48 hours targeting second to fourth instar larvae of *Spodoptera frugiperda, Spodoptera litura, Helicoverpa armigera, Tuta absoluta, Aedes aegypti,* and *Culex quinquefasciatus.*
Key findings: FTIR analysis showed Fe–O bonding at 668 cm^{-1}, while XRD revealed distinct diffraction peaks at 2θ values of 43.2°, 50.1°, and 62.1°, thereby substantiating the crystalline structure of Fe_2O_3. TEM and SEM demonstrated consistently spherical nanoparticles (~100 nm), while EDS verified iron as the predominant element. The Fe_2O_3 nanoparticles demonstrated significant dose-dependent larvicidal efficacy, with maximum mortality rates of 96.22% in *H. armigera* (LC_{50} = 216.76 µg/mL), 96.10% in *T. absoluta* (LC_{50} = 116.36 µg/mL), and 97.0% in *Ae. aegypti* (LC_{50} = 136.81 µg/mL).
Conclusions: The findings indicate the significant and extensive insecticidal efficacy of *U. lactuca*-synthesized Fe_2O_3 nanoparticles, endorsing their application as an environmentally benign nanobiopesticide.

IMPACT STATEMENT

This research illustrates the effective green manufacturing of Fe_2O_3 NPs utilizing *U. lactuca,* providing a sustainable substitute for chemical insecticides. The synthesized nanoparticles shown significant larvicidal efficacy against major agricultural and public health insect pests, such as *Spodoptera, Helicoverpa, Tuta, Aedes*, and *Culex* species. This sustainable method combines marine resources with nanotechnology to create efficient, biodegradable, and nontoxic biopesticides. The results offer considerable potential for integrated pest management approaches, decreasing reliance on synthetic pesticides and alleviating its environmental and health repercussions. This research promotes the development of marine algal nanobiotechnology in sustainable agriculture and vector management.

ARTICLE HISTORY
Received 17 March 2024
Revised 19 July 2025
Accepted 8 August 2025

KEYWORDS
Biofabrication; *Ulva lactuca*; insecticides; vector mosquitoes; biocontrol agents

1. Introduction

Insect pests present considerable risks to agriculture and public health (Belluco *et al*. 2023). Mosquitoes are notably perilous vectors, disseminating several life-threatening diseases that impose significant health and economic burdens globally, particularly in underdeveloped countries (Mohan *et al*. 2024). The two principal mosquito genera, *Aedes* and *Culex*, facilitate the transfer of pathogens responsible for diseases including dengue, malaria, chikungunya, lymphatic filariasis, and yellow fever, impacting both humans and animals (Dahmana and Mediannikov 2020, Hillary et al. 2021). *Aedes aegypti* is a principal vector for the dengue virus, with more than 5.2 million documented cases in 2019. Mortality rates have significantly escalated, particularly among younger demographics from 960 deaths in 2000 to 4,032 in 2015 (WHO 2022). Lymphatic filariasis

CONTACT Ranganathan Muthusamy rmuthusamy.dr@gmail.com PG and Research Centre in Biotechnology, MGR College, Adhiyamaan Educational Research Institution, Hosur 635 130, Tamil Nadu, India.

impacts almost 80 million individuals each year, with *Culex quinquefasciatus* responsible for nearly 30 million of these instances. In India, around 19 million individuals exhibit symptoms of filarial illness, adding to a worldwide total of 120 million cases (Ramkumar *et al*. 2023).

Agricultural pests significantly affect crop output and quality in numerous places. Significant insect pests, including *Spodoptera frugiperda*, *Spodoptera litura, Helicoverpa armigera,* and *Tuta absoluta,* inflict considerable harm on over 180 plant species, encompassing economically vital crops such as cotton, tomato, cabbage, and cauliflower (Tarusikirwa et al. 2020, Khan et al. 2022, Lateef *et al*. 2024, Narayanan 2025). Historically, pest management has predominantly depended on synthetic chemical insecticides (Kandil *et al*. 2020). Nonetheless, overutilization has resulted in numerous issues, such as the emergence of insecticide resistance, environmental pollution, and adverse impacts on non-target organisms (Arokiyaraj et al. 2014, Ali et al. 2022, Siddiqui et al. 2022, Khangura et al. 2023, Muthusamy et al. 2024). These disadvantages highlight the pressing necessity for environmentally sustainable and efficient pest management options.

Nanotechnology has emerged as a new application in the biosciences, which shown effective against insect pests by infiltrating plant tissues and serving as carriers for active substances (Khot et al. 2012, Nie *et al*. 2023, Narayanan and Prabhu 2025, Narayanan 2025, Kadry *et al*. 2025). Studies indicate that silver and graphene oxide nanoparticles can interfere with insect detoxification enzymes, leading to oxidative stress and cellular death (Altammar et al. 2023, Basheer *et al*. 2025). Metal-based nanoparticles, including Fe_2O_3, disturb insect physiology by attaching to sulfur and phosphorus in proteins and nucleic acids, thereby compromising membrane integrity.

The green synthesis of nanoparticles has attracted interest as a sustainable alternative to chemical synthesis. It improves the efficacy and stability of active chemicals in pesticides while reducing environmental risks (Gonzalez-Merino et al. 2021, Gupta *et al*. 2023). Fe_2O_3 nanoparticles are notably appealing owing to their biocompatibility, magnetic characteristics, ease of retrieval, and efficacy in biological systems (Mittal et al. 2022, Nadeem *et al.* 2022). In contrast to chemical approaches, green synthesis employs natural plant or algae extracts to decrease and stabilize nanoparticles, offering an environmentally sustainable and scalable approach for nanoparticle manufacturing (Kiwumulo et al. 2022, Bensy et al. 2022, Liu et al. 2023, Osman *et al*. 2024, Mani *et al*. 2024). These extracts are abundant in biomolecules, including flavonoids, phenols, and polysaccharides, which facilitate nanoparticle synthesis (Radulescu *et al*. 2023). Marine algae, including *Ulva lactuca*, are being increasingly investigated for these purposes (Tonelli et al. 2023, Kandasamy *et al*. 2023). This species possesses a plethora of bioactive substances, including as sulfated polysaccharides, proteins, and phenolics, which promote the production and stabilization of nanoparticles (Alboofetileh *et al*. 2021, Mohan *et al*. 2024). *Ulva lactuca* demonstrates significant antibacterial and insecticidal characteristics, positioning it as a viable choice for the eco-friendly production of Fe_2O_3 nanoparticles intended for pest management (Rima et al. 2021, Vijayakumar *et al.* 2025, Salem *et al.* 2019). Despite its extensive availability and biological potential, limited research has investigated its utilization in the synthesis of Fe_2O_3 nanoparticles for insecticidal purposes, namely targeting agricultural pests and mosquito vectors.

This research fills the gap by synthesizing Fe_2O_3 nanoparticles with *U. lactuca* extract and assessing their insecticidal effectiveness on several pest species and developmental stages. The nanoparticles were analyzed by UV-Vis spectroscopy, Fourier Transform Infrared Spectroscopy (FTIR), X-ray diffraction (XRD), scanning electron microscopy (SEM), and transmission electron microscopy (TEM) to ascertain their size, shape, and functional groups. Insecticidal experiments were performed on relevant agricultural pests and mosquito vectors to evaluate toxicity and efficacy. The research seeks to position green-synthesized Fe_2O_3 nanoparticles as a feasible, environmentally acceptable substitute for traditional chemical pesticides in sustainable pest control.

2. Materials and methods

2.1. Green algae

The *U. lactuca* was chosen for its well-documented characteristics and year-round availability. It was collected from Gulf of Mannar coastal region at the depth of 2–6 meters. The chosen seaweed was identified by Dr. V. Veeragurunathan principal scientist, CSIR-CSMSRI Marine Algae Research Station, Mandapam Campus, Tamil Nadu. India.

2.2. Aqueous extract preparation

The collected seaweed samples were immersed in a container of tap water and subsequently cleaned twice with distilled water to eliminate unwanted contaminants (Figure 1). The purified algae were shade-dried for 15 days at ambient temperature (25 ± 1 °C) with relative humidity of 50–60% prior to being pulverized

Figure 1. Seaweed *Ulva lactuca* used for the iron oxide nanoparticles synthesis.

into a fine powder using a mechanical blender (L5M-A, Silverson, USA). Approximately 25 g of seaweed powder was mixed with 250 mL of distilled water and heated to 90 °C for 30 min. The extract was filtered using Whatman no. 1 filter paper and preserved at refrigeration temperature of 4 °C till subsequent usage.

2.3. Green synthesis of Fe_2O_3-NPs

The iron oxide nanoparticles were synthesized according to the procedure outlined by Mahdavi *et al.* (2013) with some changes. Approximately 50 mL of *U. lactuca* extract was combined with an equal volume (50 mL) of 0.4 M $FeCl_3$ solution. The mixture was thoroughly agitated and positioned on the hot plate (100 °C) with continuous magnetic stirring for 45 min to monitor color changes. The sample was centrifuged at 5,000 rpm for 20 min at 4 °C to eliminate any residual aqueous extract from the freshly synthesized NPs. The aqueous mixture containing Fe_2O_3-NPs was centrifuged a second time and resuspended in double distilled water. Finally, the Fe_2O_3-NPs were ultimately dissolved in 100% ethanol prior to characterization.

2.4. Characterization of Fe_2O_3-nanoparticles

The biosynthesized seaweed iron oxide nanoparticles were characterized using several analytical techniques, including UV-visible spectroscopy, Fourier transform infrared spectroscopy (FT-IR), X-ray diffraction analysis (XRD), scanning electron microscopy (SEM), and transmission electron microscopy (TEM) and energy-dispersive X-ray analysis (EDXA). The preliminary verification of Fe_2O_3-NPs synthesis was performed utilizing UV-visible spectrometry to determine the spectral frequency range of 350–800 nm and the peaks were identified. The biomolecules responsible for the reduction of ferric chloride were determined by FT-IR analysis carried out in the range of 400–4,000 cm^{-1} (Thermo Nicolet Nexus 670). The primary elemental composition of the Fe_2O_3-NPs was ascertained using energy-dispersive X-ray (EDX) using X-ray micro-analyzer (shimadzu XRD, 6000). Hitachi H-600 scanning electron microscope (SEM and TEM) was used to examine the surface morphology, size and shape of the synthesized Fe_2O_3NPs. EDXA was employed to ascertain the elemental composition of the sample at the acceleration voltage of 20.0 kV.

2.5. Insect culture and rearing

The egg masses of *S. litura* and *H. armigera* (Accession no.NBAII-MP-NOC-01) were obtained from National Bureau of Agricultural Insect Resources live insect repository (NBAIR), Bangalore, Karnataka, India. The egg masses of *S. frugiperda* and *T. absoluta* were collected from tomato and maize fields. The samples were confirmed with Dr, Asokan R, Principal Scientist, ICAR and maintained in IIHR (Indian Institute of Horticulture Research, Bangalore, Karnataka, India). Newly molted larvae were reared on artificial diet consisting 159 g chickpea flour 150 g, 0.75 g sorbic acid, 24 g yeast powder, flax oil 6 mL, agar 8.4 g, vitamin mixture 0.02 g (thiamine, pyridoxine, and biotin), ascorbic acid 2.35 g, methl-4-hydroxy benzoate 1.5 g, distilled water 550 mL, and 0.75 g streptomycin, in accordance with the established protocol (Ahmad *et al.* 2018). *A. aegypti* and *Cx. quinquefasciatus* egg masses were provided by the Institute of Vector Control and Zoonoses (IVCZ, Hosur, Tamil Nadu, India). The newly emerged mosquito larvae were reared in a plastic tray (30 × 20 cm) covered with mosquito netting, with dog biscuits provided as their nutrition. All insect cultures were sustained at 27 ± 1 °C temperature with relative humidity of 70 ± 5% under 10:14 h light: dark photoperiod condition in PG and Research Center in Biotechnology laboratory until the appearance of adulthood.

Adult male and females were released in disposable transparent plastic jars (15 cm × 15 cm × 30 cm) at 1:3 ratios for mating and were provided with a 10% sugar solution for sustenance. Female mosquitoes were provided chick blood in 60 × 60 cm rearing cages and fresh trays were installed as ovipositor. Following hatching, uniformly sized 2nd, 3rd, and 4th instars larvae were chosen for the larval bioassays.

2.6. Artificial diet bioassay

The artificial diet bioassay was performed using the established protocol of Jafir *et al.* (2021) with few alterations. Small diet samples ($5mm^3$) were manually prepared and immersed in varying concentrations of *Ulva*

Fe_2O_3 NPs (50, 100, 150, and 200 µg/mL) before being air-dried for 20 min. Simultaneously, early 2nd, 3rd, and 4th instar larvae of each insect underwent a 1-h fasting before being introduced to their introduction into the treatment diet. Untreated larvae were maintained as a control group, receiving only water. Twenty-four hours following treatment, small quantities of untreated meals were administered to satisfy the requirements of the insect larvae. The experiment was conducted under optimal conditions, as previously mentioned, with three replicates for each concentration to minimize error. The larval mortality was assessed 48 h after treatment.

2.7. Mosquito larvicidal bioassay

The larvicidal effectiveness of particular mosquito species was assessed with slight alterations (Aziz 2023). Newly hatched early 2nd, 3rd, and 4th instar larvae were placed into a 250-mL paper cup with varying concentrations of *Ulva* Fe_2O_3 prepared for treatment (50, 100, 150, and 200 µg/mL). Larvae introduced into distilled water served as a control. Each dosage was reproduced thrice, with 25 similarly sized larvae introduced into each paper cup. After 24 h, the larvae were supplied with dog biscuits for nourishment. The larval mortality was assessed 48 h after treatment.

2.8. Data analysis

The data collected from the aforementioned experiments underwent statistical analysis, with values shown as their mean ± SE. The toxicity data were evaluated using factorial analysis of variance (one-way ANOVA) and Dunnett's multiple comparision test $P < 0.05$ for pairwise mean comparisons. Probit analysis was utilized to ascertain the lethal concentrations at LC_{50} and LC_{90} values employing the SPSS statistical software, Version 16.0 (SPSS Inc., Chicago, IL, USA).

3. Results

3.1. Synthesis of Fe_2O_3-NPs

This study concentrated on devising a biosynthetic approach for generating iron oxide nanoparticles utilizing an aqueous extract of *U. lactuca*. Figure 2(A, B) illustrates that the color of the $FeCl_3$/*Ulva* extract solutions at ambient temperature swiftly transitioned from yellow to dark brown, signifying the synthesis of Fe_2O_3 nanoparticles within the seaweed extract. The incorporation of $FeCl_3$ into the *Ulva* extract may yield sulfated polysaccharides as a predominant constituent, which, due to the presence of sulfate, hydroxyl, and aldehyde groups, could facilitate the reduction of Fe3+ and the stabilization of nanoparticles.

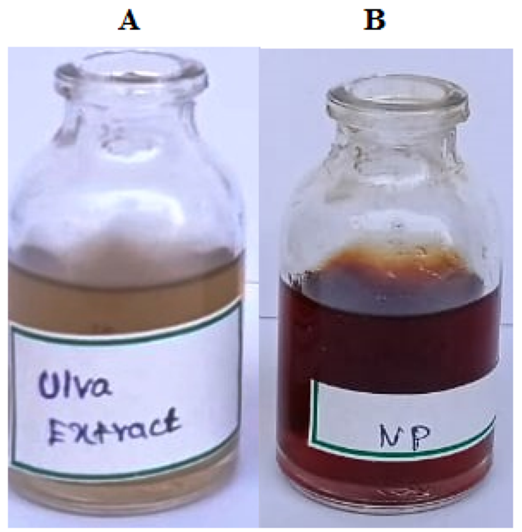

Figure 2. Fe_2O_3 NPs synthesized from *Ulva lactuca* aqueous extract. (**A**) Crude extracts. (**B**) Iron oxide nanoparticles (Brown color).

3.2. Characterization of Fe_2O_3-NPs

3.2.1. Ultraviolet-visible spectroscopy (UV-vis)

The UV-Visible spectra of aqueous extract of *U. lactuca* and synthesized Fe_2O_3-NPs are shown in Figure 3. The SPR band 1 indicates near 402 nm is a synthesized iron oxide NPs, confirming their role in the color shift and the production of Fe_2O_3-NPs. Peak 2 near 450 nm may indicates the presence of impurities in the sample.

3.2.2. Infrared spectroscopy

FTIR was employed to ascertain the functional groups of the active components by analyzing the peak values in the infrared radiation spectrum. Figure 4(A, B) illustrates the FTIR spectra of *Ulva* crude extract and Fe_2O_3-NPs synthesized using seaweed extract. The FTIR spectrum of *Ulva* extract exhibits distinctive stretching vibration bands at 668 cm^{-1} and 778 cm^{-1}, indicating the Fe-O stretch and validating the synthesis of Fe_2O_3. Supplementary peaks within 2850–2950 cm^{-1} indicated C-H bonds, but a broad peak at 3400 cm^{-1} revealed the existence of hydroxyl (OH) groups derived from *U. lactuca* bioactive chemicals that stabilize the NPs.

3.2.3. X-ray diffraction (XRD)

The crystalline structure and phase identification of nanoparticles were characterized by XRD. The XRD

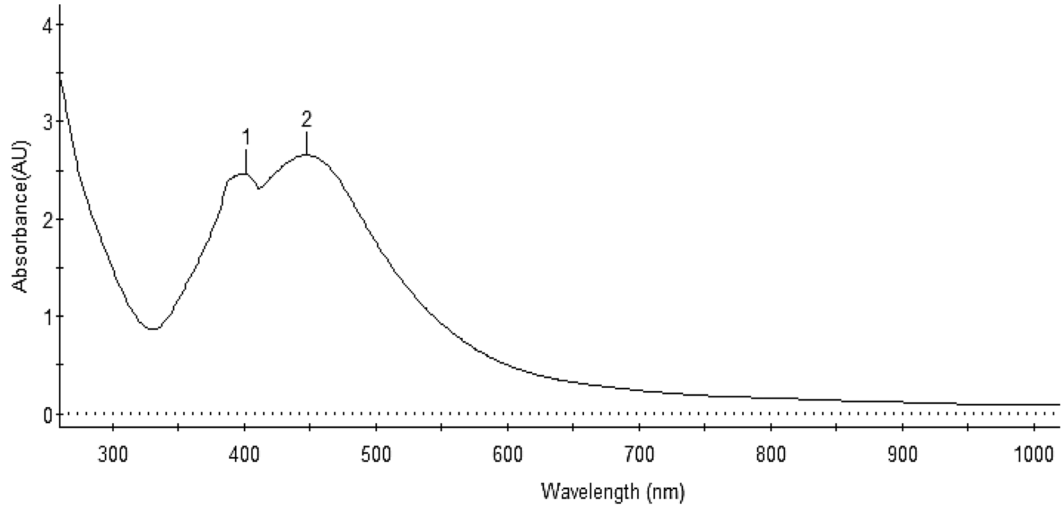

Figure 3. UV-Vis spectrophotometry showing the spectra of *U. lactuca* crude synthesized Fe_2O_3 NPs.

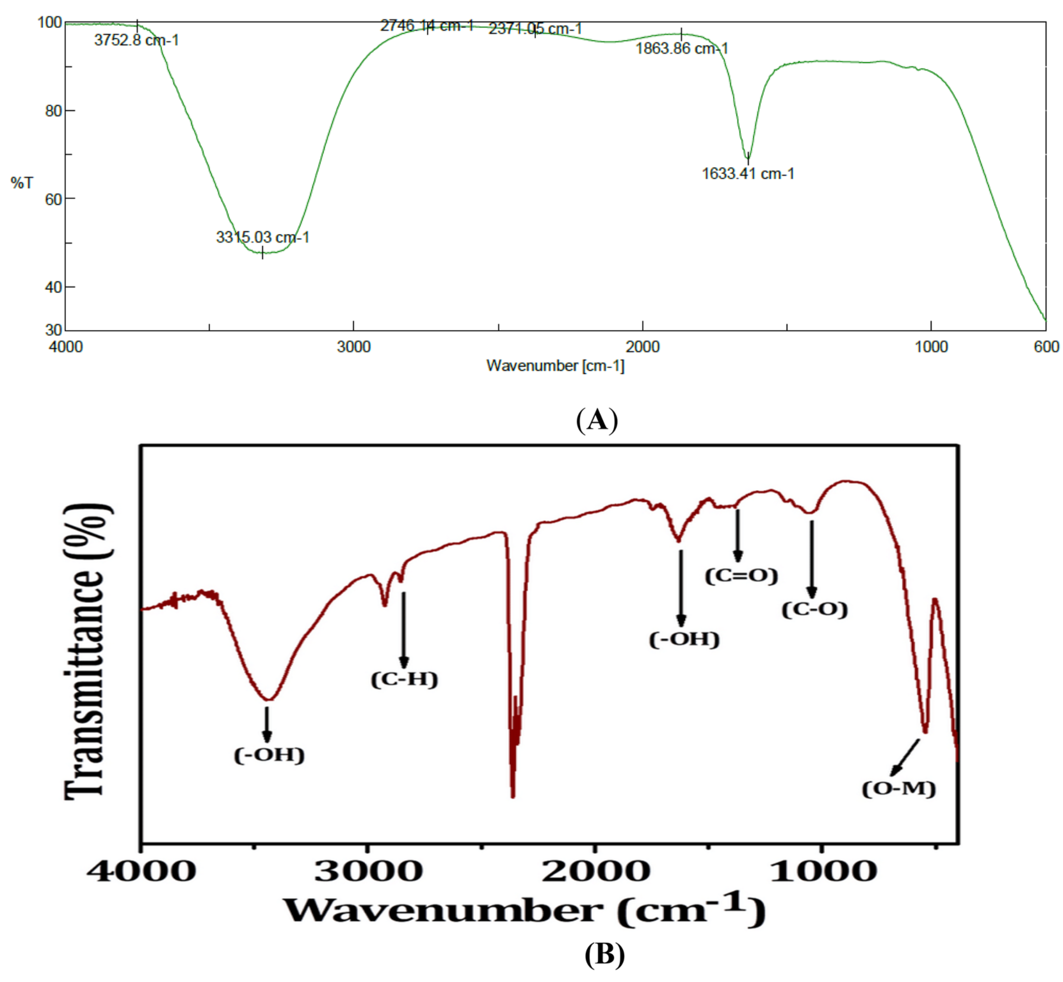

Figure 4. **(A)** FT-IR analysis of aqueous extracts of *Ulva lactuca*. **(B)** FT-IR with the peaks of *Ulva lactuca* and Fe_2O_3 nanoparticles.

pattern of the Fe_2O_3-NPs obtained from *U. lactuca* extract is shown in Figure 5. It is found that there exist strong diffraction peak with 2θ values of 25.1°, 43.2°, 50.1°, 62.1°, 68.7°, 73.1°, 80.0°, and 82.1°, corresponding to the crystal planes of (104), (110), (192), (265), (300), and (341) of crystalline Fe_3O_4-NPs, respectively.

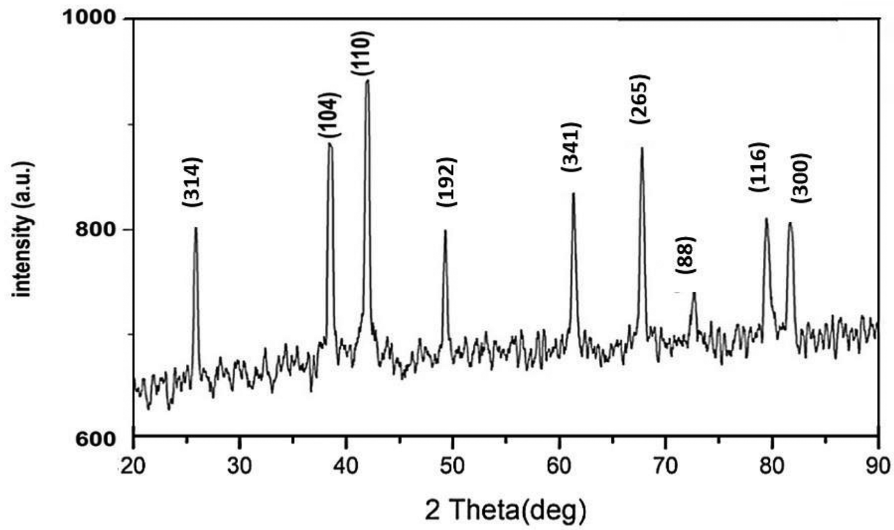

Figure 5. XRD pattern of Fe_2O_3 nanoparticles synthesized from *Ulva lactuca*.

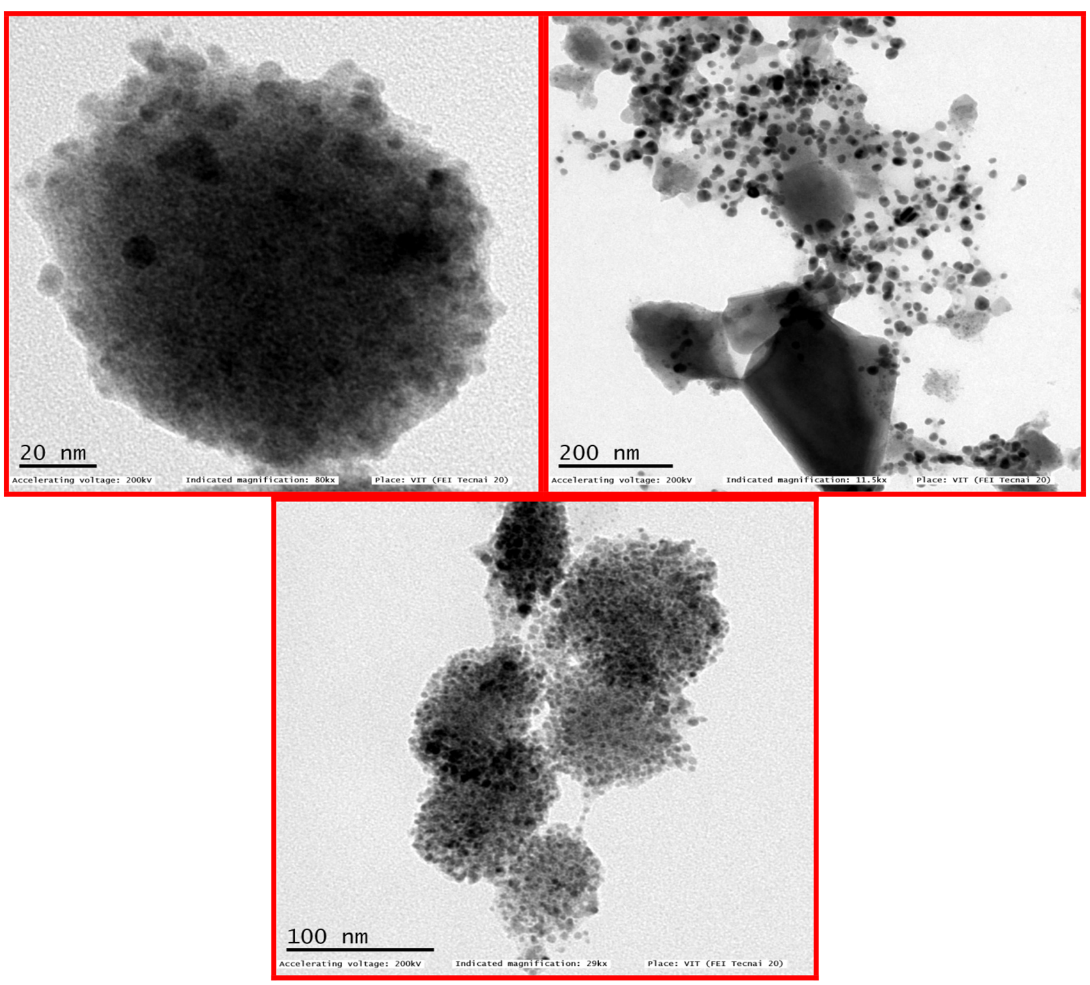

Figure 6. Transmission electron microscope (TEM) images of iron oxide nanoparticles from *Ulva lactuca* at different magnification range.

3.2.4. Transmission electron microscope (TEM)

For morphology analysis by TEM, a drop of Fe_2O_3-NPs synthesized by treating $FeCl_3$ solution with *Ulva* extract was deposited on to a TEM copper grid. The images were captured from the grid followed by drying. The images of TEM with different magnification size are shown in Figure 6. It is clear that from 100 nm the sizes of the Fe_2O_3-NPs are almost uniform and all of the particles are cubic in shape.

3.2.5. Scanning electron microscope (SEM)

The SEM image and EDaX spectra are shown in Figures 7 and 8. The SEM images confirm that the *Ulva*-derived Fe_2O_3-NPs are cubic in shape. In the EDaX spectra, the peaks around 0.8, 6.2, and 7.0 keV are related to the binding energies of Fe. Hence, the EDaX spectra of the Fe_2O_3/*Ulva* extract confirmed the presence of Fe_2O_3-NPs in the *U. lactuca* aqueous extract.

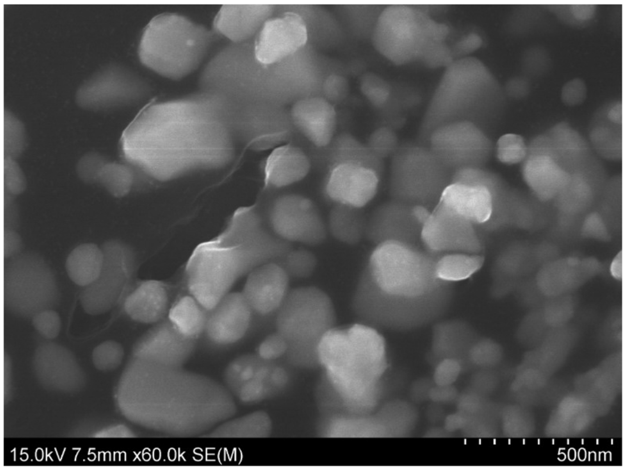

Figure 7. Scanning electron microscope (SEM) image of iron oxide nanoparticles from *Ulva lactuca*.

3.3. Mortality effect of Ulva lactuca Fe_2O_3-NPs on lepidopteran insects

The toxicological impact of *U. lactuca* Fe_2O_3-NPs against 2nd, 3rd, and 4th instar larvae of *S. frugiperda, S. litura, H. armigera*, and *T. absoluta* has been evaluated by artificial diet bioassays (Table 1.) Results showed that all the administered doses are showed increased mortality (Figures 9(A)–(C) and 10 A). The maximum concentration (200 µg/mL) of *U. lactuca* Fe_2O_3-NPs over 2nd instar showed the highest larval mortality against *S. frugiperda, S. litura, H. armigera,* and *T. absoluta* (95.17%, 92.21%, 96.22%, and 96.10%) followed by 3rd (89.11%, 87.0%, 90.10%, and 90.20%) and 4th instars (88.76%, 84.21, 85.0%, and 85.42%).

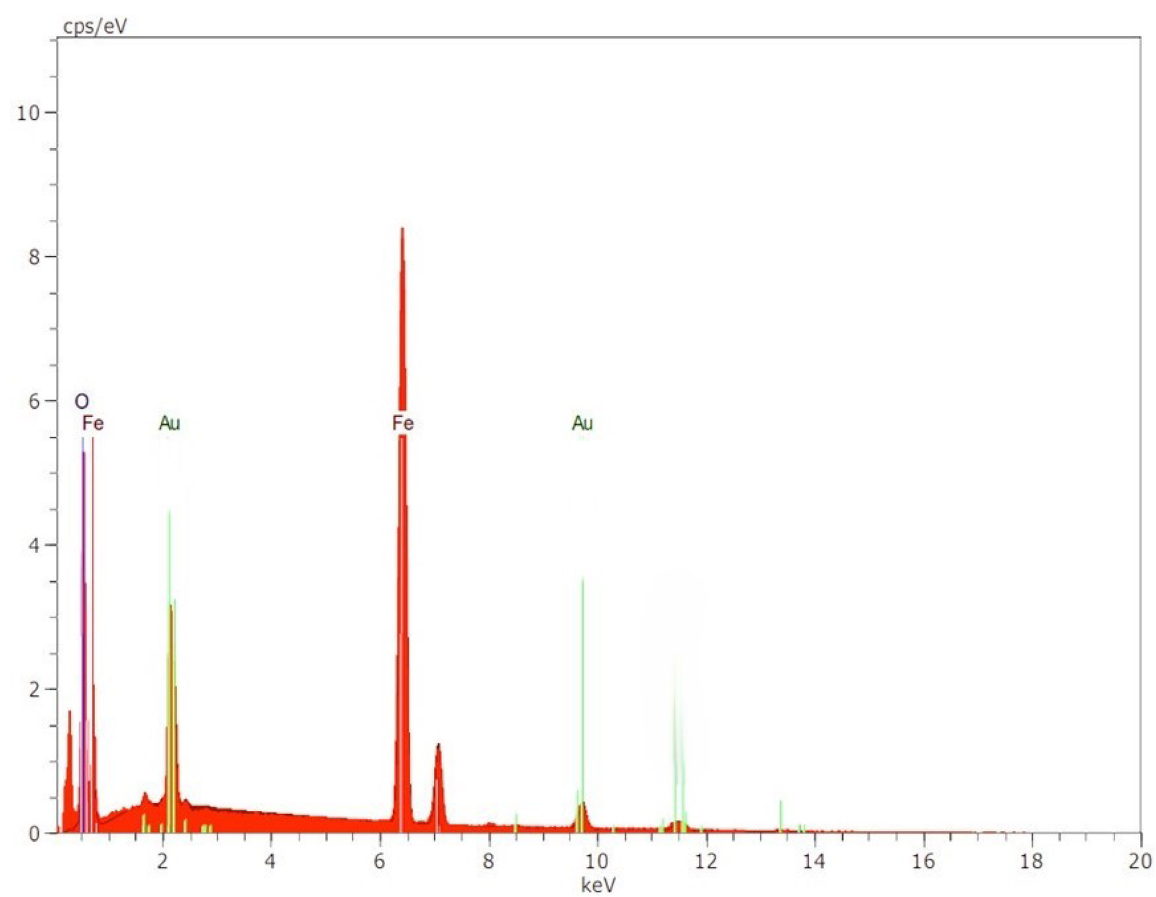

Figure 8. According to the EDaX image, the elementary composition evaluation ranges from 0 to 20 keV. Several elements are shown, and among the elements Fe (Iron oxide) is a major particle.

Table 1. Probit analysis for lethal concentration of iron oxide (Fe_2O_3) nanoparticles against different insects.

Insects	Larval Instar	LC_{50}± SE (μg/ml)	LC_{90}± SE (μg/ml)	Slope	χ^2
S. frugiperda	2nd	346.36 ± 33	1557.35 ± 2.44	0.462 ± 0.03	2.33
	3rd	425.40 ± 45	2174.54 ± 0.32	0.493 ± 0.07	7.15
	4th	532.43 ± 21	2721.21 ± 0.24	0.423 ± 0.07	7.20
S. litura	2nd	412.24 ± 44	2575.25 ± 5.41	1.212 ± 0.23	6.33
	3rd	577.31 ± 54	3144.36 ± 0.14	1.238 ± 0.30	0.40
	4th	622.43 ± 21	3421.11 ± 0.33	0.218 ± 0.67	1.62
H. armigera	2nd	216.76 ± 14	397.25 ± 24.29	1.921 ± 0.23	0.44
	3rd	397.09 ± 57	1126.55 ± 2.32	0.362 ± 2.07	0.91
	4th	412.22 ± 11	2127.36 ± 1.43	4.221 ± 0.37	5.20
T. absoluta	2nd	116.36 ± 41	197.10 ± 25.56	2.911 ± 0.23	1.08
	3rd	321.19 ± 67	1216.23 ± 7.72	2.200 ± 0.26	0.86
	4th	301.02 ± 0.9	1527.36 ± 4.13	1.112 ± 0.33	2.20
A. aegypti	2nd	136.81 ± 57	198.56 ± 16.44	2.606 ± 0.40	0.95
	3rd	295.47 ± 7.5	412.53 ± 25.65	1.993 ± 0.23	0.24
	4th	302.21 ± 5.5	521.21 ± 23.24	0.423 ± 0.07	3.04
Cx.quinquefasciatus	2nd	143.61 ± 18	323.10 ± 32.54	1.492 ± 0.30	4.39
	3rd	259.43 ± 22	474.54 ± 21.32	0.442 ± 0.27	6.15
	4th	273.81 ± 6.5	371.73 ± 20.24	0.332 ± 0.27	6.24

LC_{50} and LC_{90} lethal concentration that kills 50% and 90% of the test animal; SE, standard error; μg/ml, microgram per milliliter; χ^2, chi-square.

3.4. Mortality effect of *Ulva lactuca* Fe_2O_3-NPs on diptera insects

The mortality of *U. lactuca* synthesized Fe_2O_3 nanoparticles on *A. aegypti* and *C. quinquefasciatus* larvae is seen in Figure 10(B, C). The larval mortality was affected by increasing concentrations (50–200 μg/mL). High mortality was reported at elevated quantities of synthesized nanoparticles, with the rates of 97.0% and 93.80%. Statistical analysis of the bioassay results indicated a significant difference in larval mortality ($P < 0.05$).

4. Discussion

This study synthesized Fe_2O_3-NPs utilizing *U. lactuca* as the major source. The synthesized NPs were characterized using various analytical techniques, including UV-spectrophotometer, FTIR, XRD, TEM, SEM, and EDaX. Bio-synthesized nanopesticides effectively enhance plant pest and vector management by accurately delivering active components to specific targets in a controlled manner (Zahin et al. 2020, Vijayakumar et al. 2025). This sophisticated method provides effective solutions and reduces pesticide usage (Eldesouky *et al.* 2023). The observed color transition from yellow to dark brown in this work signifies the reduction of ferric chloride to iron oxide nanoparticles, culminating in the synthesis of Fe_2O_3-NPs. Fe_2O_3 nanoparticles are synthesized when the phytocomponents of seaweed extract act as a reducing agent on ferric chloride, therefore reducing ferric iron and yielding very stable iron nanoparticles (Bouafia and Laouini 2021, Mohanasundari *et al.* 2023).

The UV-Vis spectroscopy examination of crude and *U. lactuca* synthesized Fe_2O_3-NPs are observed within the spectral range of 402 and 450 nm. UV-Vis denotes the absorption spectrum within the UV-Vis spectrum, utilizing light in the near UV and near infrared ranges. In support of our findings, Mahdavi *et al.* (2013) found that the aqueous extract of *Sargassum muticum* facilitated the synthesis of Fe_3O_4-NPs at UV wavelengths of 402 and 415 nm. Salem *et al.* (2019) identified the absorbance peaks ranging from 402 to 415 nm for the aqueous extracts of brown seaweed (*Colpomenia sinuosa*) and red sea weed (*Pterocladia capillacea*), whereas the Fe_2O_3-NPs synthesized from *Apis mellifera* honey were measured at 350 nm (Shahid *et al.* 2023). The variations in SPR biogenesis of Fe_2O_3-NPs can be attributed to the aggregation properties of *U. lactuca* nanoparticles of varying sizes and shapes under the given conditions (Azizi *et al.* 2013).

The FTIR examination of *U. lactuca* synthesized iron oxide nanoparticles revealed unique peaks (Figure 4(A, B)), indicating the Fe-O stretch and validating the creation of Fe_2O_3, as well as the stabilization of nanoparticles by the bioactive compounds contained in *U. lactuca* (Azizi *et al.* 2013). This corroborates the mechanism in which phenolic and polysaccharide groups function as both reducing and capping agents (Sahayaraj *et al.* 2020). Comparable types of bands were seen in Fe_2O_3 nanoparticles biosynthesized from the aqueous extracts of the seaweed *C. sinuosa* (Salem *et al.* 2019).

The crystalline structure of Fe_2O_3-NPs was examined using an X-ray diffractometer. Numerous diffraction peaks were seen in the bio-fabricated iron oxide nanoparticles (Figure 5). The synthesized nanoparticles exhibited distinct diffraction peaks at (314), (104), (110), (192), (341), (265), (116), and (300) indicating their well-defined crystalline structure. The XRD

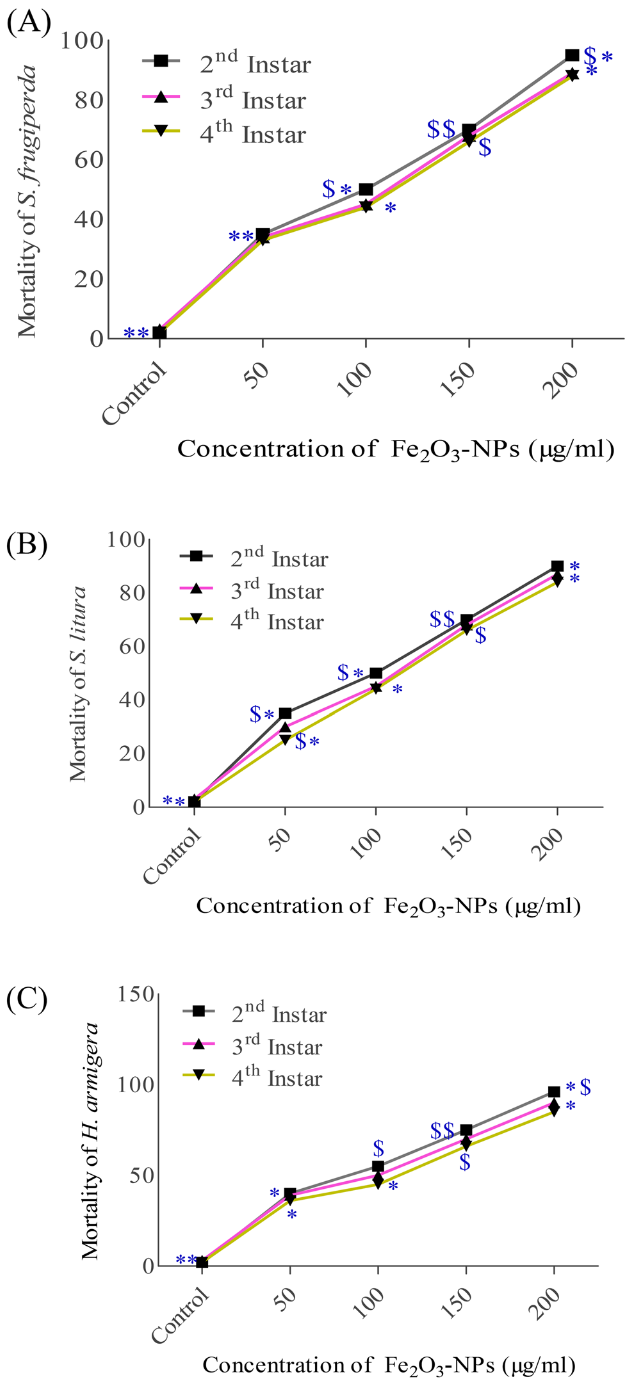

Figure 9. Percent mean mortality of *Ulva lactuca* Fe_2O_3 against S. *frugiperda* (A), *S. litura* (B), *H. armigera*, (C) 48-h post-treatment. Symbols with similar appearance are statistically significant at $P < 0.05$, different symbols are not significant (Dunnett's multiple comparision tests).

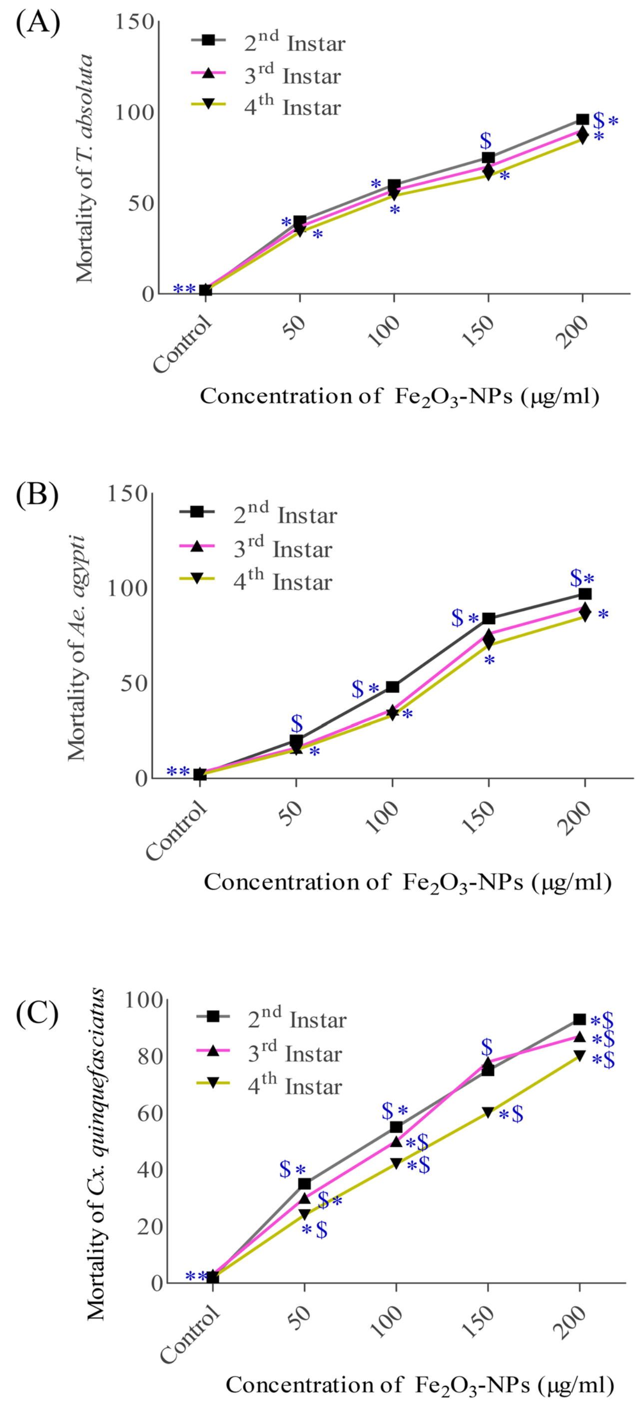

Figure 10. Percent mean mortality of *Ulva lactuca* Fe_2O_3 against *T. absoluta* (A), *Ae. aegypti* (B), *Cx. quinquefasciatus*, (C) 48-h post-treatment. Symbols with similar appearance are statistically significant at $P < 0.05$, different symbols are not significant (Dunnett's multiple comparision tests).

pattern obtained in this study aligns with previous findings on the XRD patterns of Fe_2O_3-NPs reported by Nadeem *et al*. (2022) and Ahmadi and Izanloo (2023). A significant diffraction peak was seen between 40° and 68° (2θ), confirming the ability of *U. lactuca* to synthesize iron oxide nanoparticles. Comparable outcomes in structural parameters, such as dislocation density and lattice constants, are consistent with the previous studies on biosynthesized Fe_2O_3-NPs (Chan *et al*. 2022).

TEM and SEM were utilized to ascertain the form and dimensions of the synthesized nanoparticles derived from *Ulva* seaweed. The current investigation established that the iron oxide nanoparticles produced were consistent in size and exhibited spherical and cubic shapes. Prior research indicates that the majority of nanoparticles produced using green synthesis exhibit a spherical morphology (Murugan et al. 2015, Ahmad *et al*. 2020). Bhuiyan *et al*. (2020) revealed the heterogeneous particle size distribution of iron oxide nanoparticles synthesized from *Carica* papaya leaf extract. This heterogeneity may arise from the accumulation of minute constituents of diverse bioactive reducing agents derived from plant extracts.

The toxicological impact of *U. lactuca* Fe_2O_3-NPs on 2nd, 3rd, and 4th instar larvae of agricultural pests and mosquitoes was evaluated. The peak concentration (200 µg/mL) of *U. lactuca* Fe_2O_3-NPs during the 2nd instar exhibited the highest larval mortality rates against *S. frugiperda, S. litura, H. armigera,* and *T. absoluta*. The increased mortality rate observed in this study may be ascribed to the interaction of Fe_2O_3-NPs involved in metabolic activity and protein synthesis in insects (Kalpana *et al*. 2024). A similar study demonstrated that the aqueous extract of *Nephrolepis exaltata* produced iron oxide nanoparticles exhibiting notable anti-plasmodial activity (Nadeem *et al*. 2022). Jafir *et al*. (2021) validated our results by showing that a higher concentration of *Ocimum basilicum* silver nanoparticles resulted in increased mortality rates throughout different instars of *S. litura*.

Comparable to agricultural pests, green synthesized Fe_2O_3-NPs utilizing *Grevillea robusta* leaf extract exhibited significant mortality rates against 2nd and 4th instar *Ae. aegypti* (64–96%) and *An. stephensi* (56–84%) mosquito larvae, with LC_{50} values of 238.05 ppm and 292.72 ppm, respectively (Zargham *et al*. 2023). Our research revealed an LC_{50} of 136.81 and 143.61 µg/mL for *Aedes* and *Culex* larvae, respectively. Prior research demonstrated that silver nanoparticles synthesized from the macroalgae *C. spongiosus* caused a substantial mortality rate in *An. stephensi, Ae. aegypti,* and *Cx. quinquefasciatus.* The iron oxide nanoparticles synthesized from *Grevillea robusta* leaf extract shown mortality rates of 64–96% for *Ae. aegypti* (2nd and 4th instars) and 56–84% for *Anopheles stephensi*, with LC_{50} values of 238.05 ppm and 292.72 ppm, respectively (Kumar et al. 2021, Li et al. 2022, Lippi et al. 2023, Zargham *et al*. 2023). Our work documented reduced LC_{50} values of 136.81 µg/mL for *Ae. aegypti* and 143.61 µg/mL for *Cx. quinquefasciatus*, indicating the enhanced efficacy of *U. lactuca*-mediated Fe_2O_3-NPs.

5. Conclusion

This study efficiently demonstrated the synthesis of Fe_2O_3-NPs using the green seaweed *U. lactuca*. The synthesized Fe_2O_3 nanoparticles exhibited significant dose-dependent larvicidal effectiveness ($P < 0.05$) against four agricultural pests and two mosquito vectors at various developmental stages. Among the assessed stars, the second instar larvae demonstrated the highest mortality rate, coupled with the lowest LC_{50} values, followed by the third and fourth instars. The findings highlight the potential of *U. lactuca*-derived Fe_2O_3 nanoparticles as an eco-friendly and cost-effective biocontrol agent for lepidopteran and dipteran insect species.

Acknowledgments

We are grateful to PG and Research Centre in Biotechnology and Department of Microbiology, M.G.R College, Hosur, Tamil Nadu, India, for providing a research platform. We wish to acknowledge Periyar University, Salem, Tamil Nadu, India, for technical support.

Author contributions

The research was conceptualized by all of the authors. The original draught of the manuscript was overseen by S.R and R.M. SR was in charge of keeping daily track of the project's development. R.M, M.N, AS, HS, NP, and GR assisted in the execution of the experiment as well as the interpretation of the findings. All authors read and approved the manuscript.

Availability of data and material

On reasonable request, the corresponding author will provide the datasets created and/or analyzed during the current work.

Disclosure statement

The authors declare that they have no competing interests.

Funding

The author(s) reported there is no funding associated with the work featured in this article.

ORCID

Muthusamy Ranganathan http://orcid.org/0000-0002-2650-9791

References

Ahmad, J.N., *et al.*, 2018. Molecular identification and pathological characteristics of NPV isolated from *Spodoptera litura* (Fabricius) in Pakistan. *Pakistan journal of zoology*, 50 (6), 2229–2237.

Ahmad, W., *et al.*, 2020. *Euphorbia herita* leaf extract as a reducing agent in a facile green synthesis of iron oxide nanoparticles and antimicrobial activity evaluation. *Inorganic and nano-metal chemistry*, 51, 1–8.

Ahmadi, S., and Izanloo, C., 2023. Biosynthesis of iron oxide nanoparticles at different temperatures and its application for the removal of zinc by plant mediated nanoparticles, as an eco-friendly nanoadsorbent. *Results in chemistry*, 6, 101192.

Alboofetileh, M., *et al.*, 2021. Seaweed proteins as a source of bioactive peptides. *Current pharmaceutical design*, 27 (11), 1342–1352.

Ali, I., et al., 2022. Iron and zinc micronutrients and soil inoculation of Trichoderma harzianum enhance wheat grain quality and yield. Frontiers in plant science, 13, 960948.

Altammar, K.A., 2023. A review on nanoparticles: characteristics, synthesis, applications, and challenges. *Frontiers in microbiology*, 14, 1155622.

Arokiyaraj, S., *et al.*, 2014. Rapid green synthesis of silver nanoparticles from *Chrysanthemum indicum* L and its antibacterial and cytotoxic effects: An in vitro study. *International journal of nanomedicine*, 9, 379–388.

Aziz, A., 2023. A study on the larvicidal and adulticidal potential of *Cladostepus spongiosus* macroalgae and green-fabricated silver nanoparticles against mosquito vectors. *Green processing and synthesis*, 12 (1), 20230047.

Azizi, S., *et al.*, 2013. Biosynthesis of silver nanoparticles using brown marine macroalga, *Sargassum muticum* aqueous extract. *Materials (Basel, Switzerland)*, 6 (12), 5942–5950.

Azizi, S., *et al.*, 2013. Preparation, characterization, and antimicrobial activities of ZnO nanoparticles/cellulose nanocrystal nanocomposites. *BioResources*, 8 (2), 1841–1851.

Basheer, N., et al., 2025. Diabetic retinopathy detection in retinal OCT images with fused ResNet features. International Conference on Frontier Technologies and Solutions (ICFTS), pp. 1–6.

Belluco, S., *et al.*, 2023. Insects and public health: An overview. *Insects*, 14 (3), 240.

Bensy, A.D., et al., 2022. Green synthesis of iron nanoparticles from Ulva lactuca and bactericidal activity against enteropathogens. Journal of King Saud University - science, 34 (3), 101888.

Bhuiyan, M.S.H., *et al.*, 2020. Green synthesis of ironoxide nanoparticles using *Carica papaya* leaf extract: Application for photo catalytic degradation of remazol yellow RR dye andantibacterial activity. *Heliyon*, 6 (8), e04603.

Bouafia, A., and Laouini, S.E., 2021. Plant-mediated synthesis of iron oxide nanoparticles and evaluation of the antimicrobial activity: a review. *Mini-reviews in organic chemistry*, 18 (6), 725–734.

Chan, Y.B., *et al.*, 2022. Effect of calcinations temperature on structural, morphological and optical properties of copper oxide nanostructures derived from *Garcinia mangostana* L. leaf extract. *Nanomaterials*, 12 (20), 3589.

Dahmana, H., and Mediannikov, O., 2020. Mosquito-borne diseases emergence/resurgence and how to effectively control it biologically. *Pathogens (Basel, Switzerland)*, 9 (4), 310.

Eldesouky, S.E., *et al.*, 2023. Synthesis of tungsten oxide, iron oxide and copper-doped iron oxide nanocomposites and evaluation of their mixing effects with cyromazine against *Spodoptera littoralis* (Boisduval). *ACS omega*, 8 (47), 44867–44879.

González-Merino, A.M., et al., 2021. Antifungal activity of zinc oxide nanoparticles in Fusarium oxysporum-Solanum lycopersicum pathosystem under controlled conditions. Journal of phytopathology, 169 (9), 533–544.

Gupta, D., *et al.*, 2023. Green and sustainable synthesis of nanomaterials: recent advancements and limitations. *Environmental research*, 231 (Pt 3), 116316.

Hillary, V.E., and Ceasar, S.A., 2021. Genome engineering in insects for the control of vector borne diseases. Progress in molecular biology and translational science, 179, 197–223.

Jafir, M., *et al.*, 2021. Characterization of *O. basilicum* synthesized silver nanoparticles and its relative toxicity to some insecticides against tobacco cutworm, *Spodoptera litura* Feb. (Lepidoptera; Noctuidae). *Ecotoxicology and environmental safety*, 218, 112278.

Kadry, S., *et al.*, 2025. Automatic farm insects detection using individual/fused efficientnet features. *In*: V. Bhateja, V. Abdul Hameed, S.K. Udgata, and A.T. Azar, eds. *Innovations in communication networks: sustainability for societal and industrial impact*. Singapore: Springer Nature Singapore, pp. 151–159.

Kalpana, M., *et al.*, 2024. Actinobacteria mediated synthesis of silver nanoparticles using *Streptomyces diastaticus* and their biological efficacy against human vector mosquitoes and agricultural insect pests. *Journal of natural pesticide research*, 10, 100091.

Kandasamy, S., *et al.*, 2023. 2023. The current state of algae in wastewater treatment and energy conversion: a critical review. *Current opinion in environmental science & health*, 33, 100469.

Kandil, M.A.-H., *et al.*, 2020. Comparative toxicity of new insecticides generations against tomato leafminer *Tuta absoluta* and their biochemical effects on tomato plants. *Bulletin of the national research centre*, 44 (1), 126.

Khan, A.U., et al., 2022. Lepidopteran insects' status and diversity: a review. Journal of multidisciplinary applied natural science, 3 (1), 55–80.

Khangura, R., *et al.*, 2023. Regenerative agriculture-A literature review on the practices and mechanisms used to improve soil health. *Sustainability*, 15 (3), 2338.

Khot, L.R., et al., 2012. Applications of nanomaterials in agricultural production and crop protection: a review. Crop protection, 35, 64–70.

Kiwumulo, H.F., et al., 2022. Green synthesis and characterization of iron-oxide nanoparticles using Moringa oleifera: a potential protocol for use in low and middle income countries. BMC research notes, 15 (1), 149.

Kumar, P.P., et al., 2021. Synthesis of magnesium oxide nanoparticles by eco-friendly method (green synthesis)—a review. Materials today: proceedings, 37, 3028–3030.

Lateef, A.A., *et al.*, 2024. Bacterial biota associated with the invasive insect pest *Tuta absoluta* (Meyrick). *Scientific report*, 14, 8268.

Li, R., et al., 2022. Identification of carboxylesterase genes contributing to multi-insecticide resistance in Plutella xylostella (L.). Entomologia generalis, 42 (6), 967–976.

Lippi, C.A., et al., 2023. Trends in mosquito species distribution modeling: insights for vector surveillance and disease control. Parasites & vectors, 16 (1), 302.

Liu, M., et al., 2023. Recent advances of magnetite (Fe_3O_4)-based magnetic materials in catalytic applications. Magnetochemistry, 9 (4), 110.

Mahdavi, M., *et al.*, 2013. Green biosynthesis and characterization of magnetic iron oxide (Fe_3O_4) nano-particles using seaweed (*Sargassum muticum*) aqueous extract. *Molecules (Basel, Switzerland)*, 18 (5), 5954–5964.

Mani, A., *et al.*, 2024. Neurodegenerative marine algae bioactive compounds: a viable cure to treat amyotrophic lateral sclerosis (ALS): a review. *Dubai medical journal*, 7 (3), 201–217.

Mittal, A., Roy, I., and Gandhi, S., 2022. Magnetic nanoparticles: an overview for biomedical applications. Magnetochemistry, 8 (9), 107.

Mohan R, *et al.,* 2024. Cancer Region Segmentation in Pre-Processed Breast Ultrasound Image Using VGG16 Based UNet/SegNet. In 2024 9th International Conference on Communication and Electronics Systems (ICCES) 2024 Dec 16 (pp. 1–6). IEEE.

Mohanasundari, C., *et al.*, 2023. Evaluation of antibacterial efficacy of various solvent extracts of Evolvulus alsinoides and Mucuna pruriens against multidrug resistant (MDR) pathogenic bacteria. *Applied nanoscience*, 13, 1425–1435.

Murugan, K., et al., 2015. Seaweed-synthesized silver nanoparticles: an eco-friendly tool in the fight against Plasmodium falciparum and its vector Anopheles stephensi. Parasitology research, 114 (11), 4087–4097.

Muthusamy, R., et al., 2024. Combination effect of azadirachtin and chlorantraniliprole with three synergists against a serious invasive agricultural pest Spodoptera frugiperda (Lepidoptera: Noctuidae). Biocatalysis and agricultural biotechnology, 55, 102992.

Nadeem, F., *et al.*, 2022. Characterization, antiplasmodial and cytotoxic activities of green synthesized iron oxide nanoparticles using *Nephrolepis exaltata* aqueous extract. *Molecules (Basel, Switzerland)*, 27 (15), 4931.

Narayanan, M., 2025. An evaluation of antibacterial, antioxidant, and biocompatibility (hemocompatibility) nature of green synthesized ZnONPs: An In-vitro approach. *Dubai medical journal*, 8 (1), 1–11.

Narayanan, M., and Prabhu, N., 2025. The effect of bioactive compounds in multiple sclerosis as the adjuvant immunomodulatory: a comprehensive review. *Caspian journal of neurological sciences*, 11 (3), 185–197.

Nie, D., *et al.*, 2023. Nanoparticles: a potential and effective method to control insect-borne diseases. *Bioinorganic Chemistry and Applications*, 2023, 5898160–5898113.

Osman, A.I., *et al.*, 2024. Synthesis of green nanoparticles for energy, biomedical, environmental, agricultural, and food applications: a review. *Environmental chemistry letters*, 22 (2), 841–887.

Radulescu, D.M., *et al.*, 2023. Green synthesis of metal and metal oxide nanoparticles: a review of the principles and biomedical applications. *International journal of molecular sciences*, 24 (20), 15397.

Ramkumar, G., *et al.*, 2023. Overexpression of cytochrome P450 and esterase genes involved in permethrin resistance in larvae and adults *of Culex quinquefasciatus*. *Parasitology research*, 122 (12), 3205–3212.

Rima, M., et al., 2021. Comparative study of the insecticidal activity of a high green plant (Spinacia oleracea) and a chlorophytae alga (Ulva lactuca) extracts against Drosophila melanogaster fruit fly. Annales pharmaceutiques francaises, 79 (1), 36–43.

Sahayaraj, K., *et al.*, 2020. Green synthesis of silver nanoparticles using dry leaf aqueous extract of *Pongamia glabra* Vent (Fab.), characterization and phyto fungicidal activity. *Environmental nanotechnology, monitoring and management*, 14, 100349.

Salem, D.M., *et al.*, 2019. Biogenic synthesis and antimicrobial potency of iron oxide (Fe_3O_4) nanoparticles using algae harvested from the Mediterranean Sea, Egypt. *Egyptian journal of aquatic research*, 45 (3), 197–204.

Shahid, H., *et al.*, 2023. Synthesis, characterization, and biological properties of iron oxide nanoparticles synthesized from *Apis mellifera* Honey. *Molecules (Basel, Switzerland)*, 28 (18), 6504.

Siddiqui, J.A., et al., 2022. Insights into insecticide-resistance mechanisms in invasive species: Challenges and control strategies. Frontiers in physiology, 13, 1112278.

Tarusikirwa, V.L., et al., 2020. Tuta absoluta (Meyrick) (Lepidoptera: Gelechiidae) on the "Offensive" in Africa: prospects for integrated management initiatives. Insects, 11 (11), 764.

Tonelli, F., et al., 2023. Algae-based green AgNPs, AuNPs, and FeNPs as potential nano remediators. Green processing and synthesis, 12 (1), 20230008.

Vijayakumarr, K., et al., 2025. Classification of Benign/Malignant Digital Mammogram Images using Deep Learning Scheme. 2025 International Conference on Frontier Technologies and Solutions (ICFTS), pp. 1–6, doi: 10.1109/ICFTS62006.2025.11031579

WHO, 2022. Laboratory testing for Zika virus and dengue virus infections: interim guidance, 14 (No. WHO/ZIKV_DENV/LAB/2022.1). Geneva: World Health Organization.

Zahin, N., et al., 2020. Nanoparticles and its biomedical applications in health and diseases: special focus on drug delivery. Environmental science and pollution research international, 27 (16), 19151–19168.

Zargham, F., *et al.*, 2023. Larvicidal activity of green synthesized iron oxide nanoparticles using *Grevillea robusta* Cunn. Leaf extract against vector mosquitoes and their characterization. *Experimental parasitology*, 252, 108586.